RESEARCH ARTICLE

Long-term adaptation of global transcription and metabolism in the liver of high-fat diet-fed C57BL/6J mice

Gyeong-Min Do[1], Hea Young Oh[2]*, Eun-Young Kwon[3], Yun-young Cho[3], Su-kyung Shin[3], Hae-Jin Park[3], Seon-Min Jeon[1], Eunjung Kim[4], Cheol-Goo Hur[2], Tae-Sun Park[5], Mi-Kyung Sung[1], Robin A. McGregor[1] and Myung-Sook Choi[1,3]*

[1] Center for Food and Nutritional Genomics Research, Kyungpook National University, Daegu, Republic of Korea
[2] Omics Integration Research Center, KRIBB, Yuseong-gu, Daejeon, Republic of Korea
[3] Department of Food Science and Nutrition, Kyungpook National University, Daegu, Republic of Korea
[4] Department of Food Science and Nutrition, Catholic University of Daegu, Gyeongsan, Republic of Korea
[5] Department of Food Science and Nutrition, Yonsei University, Seoul, Republic of Korea
[6] Department of Food Science and Nutrition, Sookmyung University, Seoul, Republic of Korea

Scope: This study investigated the global transcriptional and metabolic changes occurring at multiple time points over 24 wk in response to a high-fat diet (HFD).
Methods and results: C57BL/6J mice were fed a HFD or normal diet (ND) over 24 wk. HFD-fed mice developed early clinical indicators of obesity-related co-morbidities including fatty liver, insulin resistance, hyperglycemia and hypercholesterolemia. Time-course microarray analysis at eight time points over 24 wk identified 332 HFD responsive genes as potential targets to counteract diet-induced obesity (DIO) and related co-morbidities. Glucose regulating enzyme activity and gene expression were altered early in the HFD-fed mice. Fatty acid (FA) and triglyceride (TG) accumulation in combination with inflammatory changes appear to be likely candidates contributing to hepatic insulin resistance. *Cidea* seemed to be one of representative genes related to these changes.
Conclusion: Global transcriptional and metabolic profiling across multiple time points in liver revealed potential targets for nutritional interventions to reverse DIO. In future, new approaches targeting HFD responsive genes and hepatic metabolism could help ameliorate the deleterious effects of an HFD and DIO-related complication.

Received: January 28, 2011
Revised: February 24, 2011
Accepted: March 8, 2011

Keywords:
Diet-induced obesity / Insulin resistance / Metabolic profile / Microarray / Transcriptional response

1 Introduction

Obesity is a worldwide health problem characterized by excessive body fat, which can lead to long-term health consequences such as type 2 diabetes (T2D), fatty liver, atherosclerosis and other associated co-morbidities [1–4]. Prolonged high-fat diet (HFD) feeding in rodents has been strongly associated with the development of oxidative stress, inflammation and insulin resistance [5, 6]. However, the timing of the molecular and pathophysiological changes in response to a HFD is still not fully understood. The induction of hepatic insulin resistance and chronic inflammation by high-fat feeding may play a role in the pathogenesis of T2D and other obesity-related co-morbidities such as hepatic steatosis via alterations in lipid and glucose homeostasis [7].

With the emergence of the genome era and advances in microarray technology, it is now possible to gain unprecedented insight into the hepatic transcriptional changes occurring during the development of diet-induced obesity

Correspondence: Professor Myung-Sook Choi, Department of Food Science and Nutrition, Kyungpook National University, 1370 Sank-Yuk Dong Puk-Ku, Daegu 702-701, Korea
E-mail: mschoi@knu.ac.kr
Fax: +82-53-950-6229

Abbreviations: ACAT, acyl-COA: cholesterol acyltransferase; **CAT,** catalase; **CPT,** carnitine palmitoyl transferase; **HDL-C,** HDL-cholesterol; **DIO,** diet-induced obesity; **FA,** fatty acid; **FAS,** fatty acid synthase; **FFA,** free fatty acid; **G6Pase,** glucose-6-phosphatase; **GK,** glucokinase; **HFD,** high-fat diet; **IPGTT,** intraperitoneal glucose tolerance test; **ME,** malic enzyme; **ND,** normal diet; **PEPCK,** phosphoenolpyruvate carboxykinase; **SOD,** seroxide dismutase; **T2D,** type 2 diabetes; **TBARS,** thiobarbituric acid reactive substances; **TG,** triglyceride

*These authors contributed equally to this work.

(DIO) [8]. Previous microarray studies have used various murine DIO models, which have revealed HFD feeding causes a significant induction of inflammation-related genes and suppression of lipid metabolism genes [9–14]. Comparison between these studies is difficult due to differences in age, sex, diet, duration and animal sub-strain. Furthermore, past studies have used unusually HFDs, which do not reflect human dietary consumption [9–14]. Therefore, the temporal changes in gene expression occurring during prolonged physiologically relevant high-fat feeding remain to be fully elucidated. Past microarray studies have reported differences in both the early and late transcriptional response to DIO over 16 wk [9, 14]. Mice fed an HFD may develop compensatory responses to resist the increase in energy balance, but a more prolonged HFD diet may disrupt adaptation, hence essential longer term DIO studies are undertaken.

We provide the first report investigating the time-dependent global transcriptional changes, in combination with metabolic profiling, during long-term physiological HFD feeding in C57BL/6J mice compared to age-matched normal diet (ND)-fed controls.

2 Materials and methods

2.1 Animals

Three hundred and sixty male inbred C57BL/6J mice were obtained from the Jackson Laboratory (Bar Harbor, ME, USA) at 4 wk of age. All the mice were individually housed under a constant temperature (24°C) and 12-h light/dark cycle, fed the AIN-76 semi-purified diet for a 1 wk acclimation period after arrival and then randomly divided into an ND and an HFD group, with 18 mice per group (Fig. 1). After the acclimation period, the HFD group was fed the AIN-76 semi-purified diet consisting of 20% fat and 1% cholesterol (American Institute of Nutrition, 1977). Every 2–4 wk, after a 12-h fast, blood samples were drawn from the inferior vena cava. Blood was collected in heparin-coated tubes, centrifuged at $1000 \times g$ for 15 min at 4°C and then stored at −70°C. Mice were anaesthetized and sacrificed at 0, 2, 4, 6, 8, 12, 16, 20 and 24 wk (Fig. 1). The liver and other organs were then removed, rinsed, weighed, immediately frozen in liquid nitrogen and stored at −70°C until further analysis. The current study protocol was approved by the Ethics Committee for animal studies at Kyungpook National University, Republic of Korea.

2.2 Analyses of plasma and hepatic lipids

Enzymatic assays for plasma total cholesterol (Total-C), HDL-cholesterol (HDL-C) and triglycerides (TG) were performed using enzymatic kits (Asan Pharm, Korea) based on the cholesterol oxidase method and the lipase-glycerol phosphate oxidase method. The hepatic lipids were extracted using procedures described previously [15] and dried lipid residues were dissolved in isopropanol. Hepatic cholesterol and TG concentrations were conducted using the same enzymatic kit used for plasma analyses [16]. LDL-cholesterol and atherogenic index were calculated as (Total-cholesterol)(HDL-cholesterol)(Triglycerides/5) and (Total-cholesterol)(HDL-cholesterol)/HDL-C, respectively.

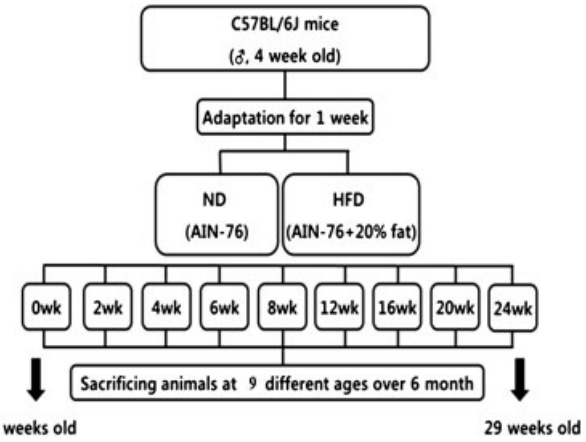

Figure 1. Experimental design to determine transcriptional and metabolic changes during the pathogenesis of diet-induced obesity.

2.3 Blood glucose, intraperitoneal glucose tolerance test (IPGTT) and plasma insulin

Every 2 wk, after a 12-h fast, whole blood was obtained from the tail veins and fasting blood glucose measured using a glucose analyzer (GlucDr supersensor, Allmedicus, Korea). The IPGTT was performed at weeks 16, 20 and 24. After a 12-h fast, mice were injected intraperitoneally with glucose (0.5 g/kg body weight), and blood glucose levels were determined from the tail vein at 0, 30, 60 and 120 min. Radioimmunometric assays were used for the measurement of plasma insulin concentration (Milliplex^{TM} $_{MAP}$ Mouse endocrine kit, Millipore).

2.4 Preparation of hepatic subcellular fractions

Hepatic microsomes were prepared to separate mitochondrial and cytosolic fractions as previously described [17]. The mitochondrial fraction was used for the measurement of glucose-6-phosphatase (G6Pase), carnitine palmitoyl transferase (CPT) and β-oxidation activity. The resulting cytosolic fraction was used for the measurement of glucokinase (GK), phosphoenolpyruvate carboxykinase (PEPCK) activity and fatty acid synthase (FAS). The microsomal pellets were then redissolved in 1 mL of homogenization buffer without DTT

and the protein concentrations were determined using the Bradford method.

2.5 Hepatic enzyme activities and glycogen concentration

Spectrophotometric assays were used to determine GK, G6Pase and PEPCK activity as previously published [18–20]. FAS and CPT activity were measured as previously described [21, 22]. Fatty acid (FA) β-oxidation was determined by monitoring the reduction of NAD to NADH at 340 nm [23]. Malic enzyme (ME), phosphatidate phosphohydrolase (PAP) and glucose-6-phosphate dehydrogenase (G6PD) activities were measured according to procedures previously described [24–26]. Microsomal HMG-CoA and acyl-COA: cholesterol acyltransferase (ACAT) activities were measured with [^{14}C]-HMG-CoA and [^{14}C]-Oleoyl CoA as substrates, respectively [27, 28].

2.6 Histopathological analysis of hepatic fat accumulation

Hepatic tissue was removed from each mouse and cleaned free of connective tissues. Samples were then fixed in 10% v/v paraformaldehyde/PBS and embedded in paraffin for staining with hematoxylin and eosin (H&E). The stained area was viewed using a microscope at a magnification of 200 ×.

2.7 Hepatic antioxidant enzyme activities and oxidative stress

Seroxide dismutase (SOD) activity and catalase (CAT) activity were measured using spectrophotometry using previously established methods [29, 30]. To measure CAT activity, the disappearance of hydrogen peroxide was monitored at 240 nm for 5 min and a molar extinction coefficient of 0.041 $mM^{-1}\,cm^{-1}$ was used to calculate CAT activity [30]. GSH-Px activity was measured using the method of Paglia and Valentine [31]. Thiobarbituric acid reactive substances (TBARS) were measured using the method of Ohkawa et al. [32].

2.8 RNA preparation and quality control

Total RNA was extracted from the liver using a TRIZOL reagent (Invitrogen, USA) according to the manufacturer's instructions. DNase digestion was used to remove any DNA contamination and RNA was re-precipitated in ethanol to ensure no phenol contamination. For quality control, RNA purity and integrity were evaluated using the Agilent 2100 Bioanalyzer (Agilent Technologies, USA). Six pooled RNA sample sets were constructed with 18 individual samples from the ND and HFD-fed mice as described previously [16]. RNA was stored at −70°C prior to further analysis by microarray and RT-qPCR.

2.9 RT-qPCR

Total RNA (1 μg) was reverse-transcribed into cDNA using the QuantiTect® reverse transcription kit (Qiagen, Germany). Then, mRNA expression was quantified by real-time quantitative PCR, using the SYBR green PCR kit (Qiagen, Germany) and the CFX96TM real-time system (BIO-RAD). Gene specific mouse primers were used to detect *Cfd*, *Lpl*, *Gck*, *Cidea*, *Pck1* and *Gapdh* (Supporting Information Table S2). Cycle thresholds were determined based on SYBR green emission intensity during the exponential phase. Ct data were normalized using *Gapdh*, which was stably expressed in both HFD- and ND-fed mice. Relative gene expression was calculated with the $2^{-\Delta\Delta Ct}$ method [33].

2.10 Microarray analysis

Total RNA was amplified and purified using the Ambion Illumina RNA amplification kit (Ambion, USA) to yield biotinylated cRNA. A total of 750 ng biotinylated cRNA per sample was hybridized to Illumina MouseWG-6 v2 Expression BeadChips (Illumina, USA) for 16 h at 58°C according to the manufacturer's instructions. Hybridized arrays were washed and stained with Amersham fluorolink streptavidin-Cy3 (GE Healthcare Bio-Sciences, UK) following the standard protocol in the bead array manual. The quality of hybridization and overall chip performance was determined by visual inspection of both internal quality controls and the raw scanned data in the Illumina BeadStudio software. Probe signal intensities significantly higher than background intensities were determined (detection p-value <0.05), but probe signal data were not filtered to preserve probes with low expression at different time points. Probe signal intensities were quantile normalized and log transformed. Microarray analysis was performed in the ArrayAssist® software (Stratagene, USA), Bioconductor and R programing language. LIMMA was used to determine significant differentially expressed genes (HFD responsive genes) between HFD- and ND-fed mice at each time point based on FDR $<5\%$, Benjamin and Hochberg adjusted p-value <0.05 and log fold change >1 [34] (Supporting Information 1). To identify the biological processes associated with the HFD responsive genes over the entire time-course, the DAVID Functional Annotation Clustering tool was applied [35]. DAVID is a comprehensive tool based on gene ontologies and facilitates the identification of enriched biological themes within the HFD responsive genes. Gene ontology analysis was conducted on the HFD responsive genes identified as upregulated or downregulated at each time point (Supporting Information 1).

2.11 Statistical analysis

The parameter values were all expressed as the mean ± standard error of the mean (SEM). Significant differences in plasma glucose, lipids and hepatic enzyme activities at each time point between the HFD and ND groups were determined using one-way analysis of variance (ANOVA) in SPSS (SPSS, USA). Any significant between group differences identified at each time point were analyzed further using Duncan's multiple-range post hoc test. The results were considered statistically significant at $p<0.05$.

3 Results

3.1 Time-dependent growth and organ weights

Significant body weight gain and FER were observed after 4 wk in the HFD group, although liver weight were significantly increased after only 2 wk in the HFD group (Fig. 2A–C). Fat depots including interscapular, epididymal, visceral and subcutaneous fat were all significantly increased in the HFD group compared to the ND group (data not shown). Liver tissue staining revealed clear differences in hepatic lipid droplet accumulation from week 2 in the HFD group, which indicated the early development of fatty liver (Fig. 2D).

3.2 Time-course of changes in fasting blood glucose, glucose tolerance, insulin concentration and hepatic glucose regulatory enzyme activities

Fasting blood glucose and insulin concentrations were markedly elevated from week 16 in the HFD group (Fig. 3A and B). IPGTT revealed significantly impaired glucose tolerance from week 16 (Fig. 3C). HOMA-IR was significantly elevated from week 16 in the HFD group (Fig. 3D), indicating increased insulin resistance. Hepatic GK activity was significantly elevated in the HFD group compared to the ND group from week 4 (Fig. 3E). Glycogen was consistently elevated in the HFD group from week 12 to week 24 (Fig. 3F). G6Pase activity was also suppressed in the HFD group, in particular from week 16 to week 24 (Fig. 3G). Hepatic PEPCK activity was consistently lower in the HFD group from week 2 to week 24 (Fig. 3H).

3.3 Time-course of changes in hepatic lipid metabolism and plasma lipid metabolites

Significantly elevated hepatic TG concentrations were observed in the HFD group after 2 wk, while hepatic cholesterol and free fatty acid (FFA) concentrations were significantly elevated after 4 wk in the HFD group. Hepatic TG, cholesterol and FFA concentrations increased progressively in the HFD group over 24 wk compared to the ND group (Fig. 4A–C). Interestingly, despite early increases in hepatic cholesterol, plasma total cholesterol concentration was significantly elevated in the HFD group after 6 wk (Fig. 4D). In addition, despite the significant increases in hepatic TG and FFA observed over the entire 24 wk, no differences in plasma TG and FFA levels were detectable between the HFD group and ND group at any time points (data not shown). Plasma LDL-C concentration consistently increased from week 6 in the HFD group while plasma HDL-C concentrations only increased later at week 12 (Fig. 4E). Interestingly, there was a dramatic increase in both plasma LDL-C and HDL-C concentrations in the HFD group at 24 wk. The atherogenic index in the HFD group was significantly higher at week 8, and it had risen again after week 20 (Fig. 4F).

FA oxidation enzyme activity appeared to be continuously downregulated in the HFD group over 24 wk (Table 1). CPT activity was significantly lower in the HFD group compared to ND group after week 2. β-Oxidation activity was progressively decreased from week 4 in the HFD group. Over 24 wk, both CPT activity and β-oxidation activity progressively decreased in the HFD group compared to the ND group (Table 1).

ME activity was significantly lower in the HFD group between week 2 and week 8, thereafter ME activity was similar (Table 1); in contrast, FAS activity was not different between groups (data not shown). Activity of glucose-6-phosphate dehydrogenase was significantly suppressed over the entire 24 wk in the HFD group compared to the ND group (Table 1). Activity of phosphatidate phosphohydrolase, a TG synthesis enzyme, was also significantly suppressed in the HFD group after week 2, and remained consistently lower in the HFD group except at week 24 (Table 1). ACAT activity was significantly elevated in the HFD group compared to ND group between weeks 4 and 6, weeks 8 and 12 and at week 24 (Table 1). HMG-CoA enzyme activity was significantly decreased in the HFD group from week 2 until week 16, and thereafter was similar to the ND group (Table 1).

3.4 Time-course of changes in hepatic antioxidant enzyme activity

Hepatic antioxidant enzyme activities were altered in response to an HFD. CAT activity was significantly elevated at week 2, and later between weeks 12 and 20 in the HFD group compared to the ND group. GSH-Px activity was consistently higher both early between weeks 2 and 4 and later between weeks 12 and 24 in the HFD group (Table 2). In contrast, SOD activity was altered later in response to HFD feeding, SOD activity

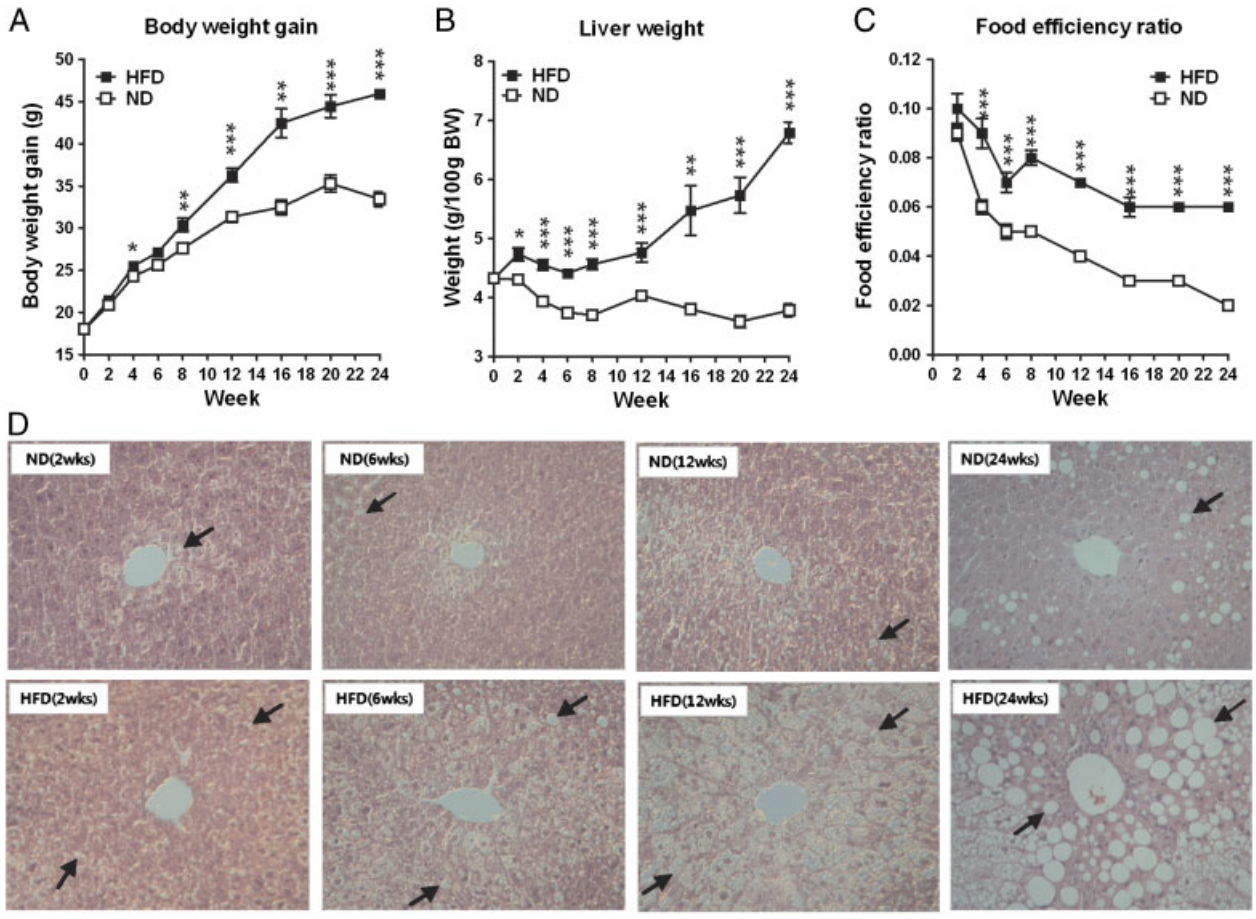

Figure 2. Time-dependent effect of a HFD on (A) body weight gain, (B) liver weight, (C) food efficiency and (D) hepatic lipid droplet accumulation in fixed tranverse liver sections stained with hematoxylin and eosin. Original magnification 200 ×. Arrows indicate example lipid droplets. Data shown as mean ± SE. Significant differences between HFD versus ND are indicated. $^{*}p<0.05$. $^{**}p<0.01$. $^{***}p<0.001$. ND, normal diet; HFD, high-fat diet; FER, food efficiency ratio.

significant increased between weeks 12 and 24 (Table 2). Activity of GR was unaltered in response to HFD feeding (data not shown). Concentration of TBARS was significantly elevated between weeks 12 and 16 in the HFD group (Table 2).

3.5 Time-dependent transcriptional changes in liver and RT-qPCR validation

Overall, 332 unique genes were found to be responsive to HFD at one or more time points (Supporting Information 1). Of these 332 HFD responsive genes, 91 genes were downregulated and 241 genes were upregulated (Table 3). Five genes including *Lpl*, *Cidea*, *Gck*, *Cfd* and *Pck1* were selected for further validation by RT-qPCR (Fig. 5). The magnitude of the fold change determined using RT-qPCR tended to be greater than fold changes determined from the microarrays, although this is not an unusual observation, as RT-qPCR is well recognized as being more sensitive than microarray for quantification of fold change in gene expression.

Functional annotation clustering revealed the biological processes and pathways that are associated with the 332 HFD responsive genes (Supporting Information 1). The biological processes consistently enriched among the upregulated genes across all time points, in response to HFD feeding, were associated with immune and inflammatory system function (Fig. 6).

While the biological processes consistently enriched among downregulated genes, in response to HFD feeding, were linked to lipid and cholesterol metabolism. Genes linked to the metabolism of xenobiotics were both up and downregulated in the HFD group, indicating both positive and negative regulation of antioxidant metabolism during the course of DIO (Fig. 6). Further in-depth analysis of the functional gene ontologies associated with HFD responsive genes at each time point confirmed the enrichment of genes involved in the immune and inflammatory response at every time point (Supporting Information 1).

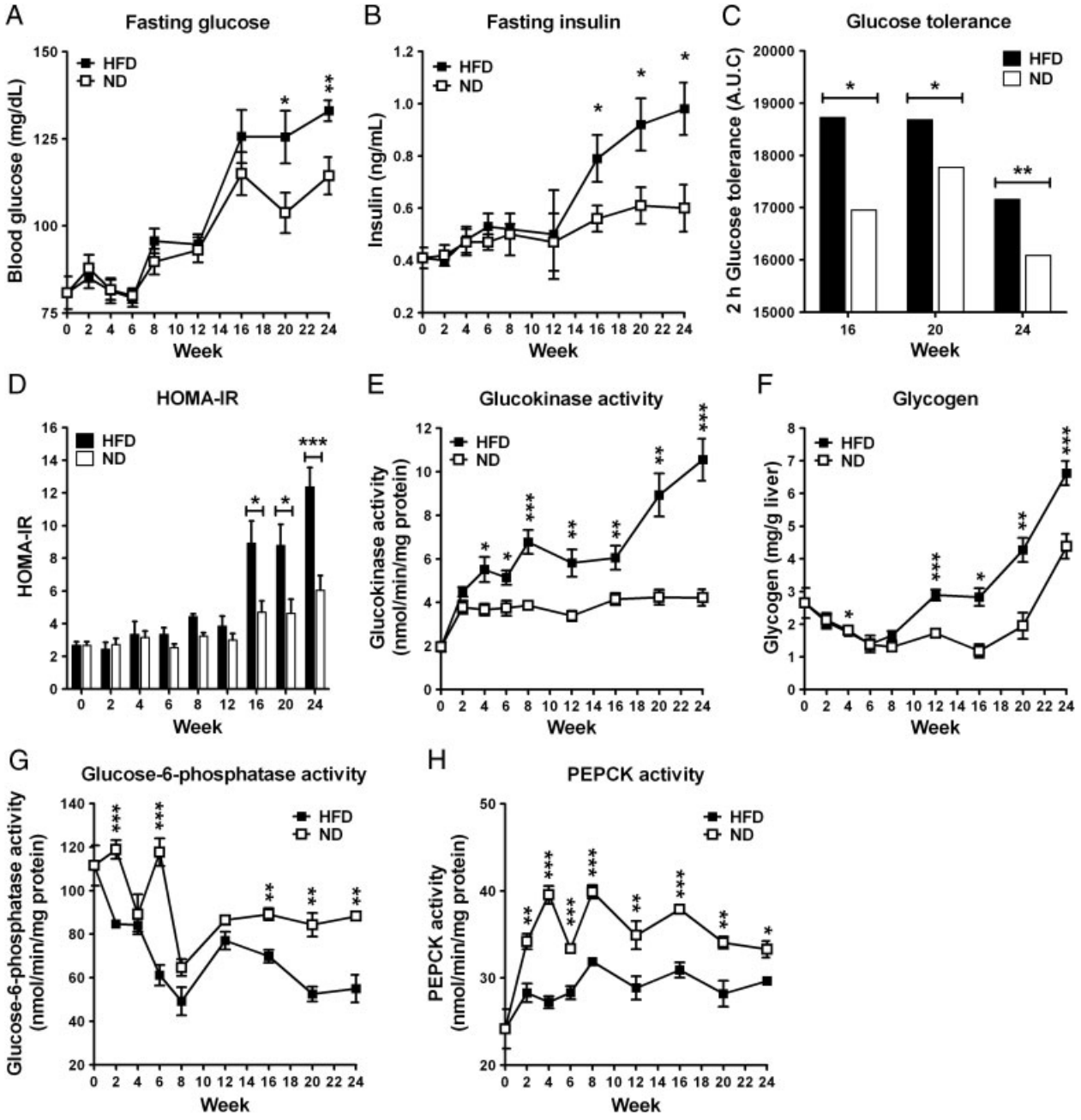

Figure 3. Time-dependent effect of a HFD on (A) fasting blood glucose, (B) fasting insulin, (C) glucose tolerance, (D) HOMA-IR, (E) glucokinase activity, (F) glycogen, (G) glucose-6-phosphate activity and (H) PEPCK activity in C57BL/6J mice. Data shown as mean ± SE Significant differences between HFD versus ND are indicated. $^{*}p<0.05$. $^{**}p<0.01$. $^{***}p<0.001$. ND, normal diet; HFD, high-fat diet; AUC, area under the curve.

4 Discussion

In the present study, changes in global transcription and metabolic profiles were analyzed at multiple time points to identify concomitant changes in gene expression and metabolism during the development of DIO and co-morbidities in C57BL/6J mice. Early signs of fatty deposition in liver were present after only 2 wk in the HFD group compared to age-matched ND group. However, early biomarkers of T2D pathogenesis including fasting glucose, impaired glucose tolerance and insulin resistance occurred later after 16 wk in the HFD-fed mice. Atherosclerosis index was consistently increased only after 20 wk in HFD group.

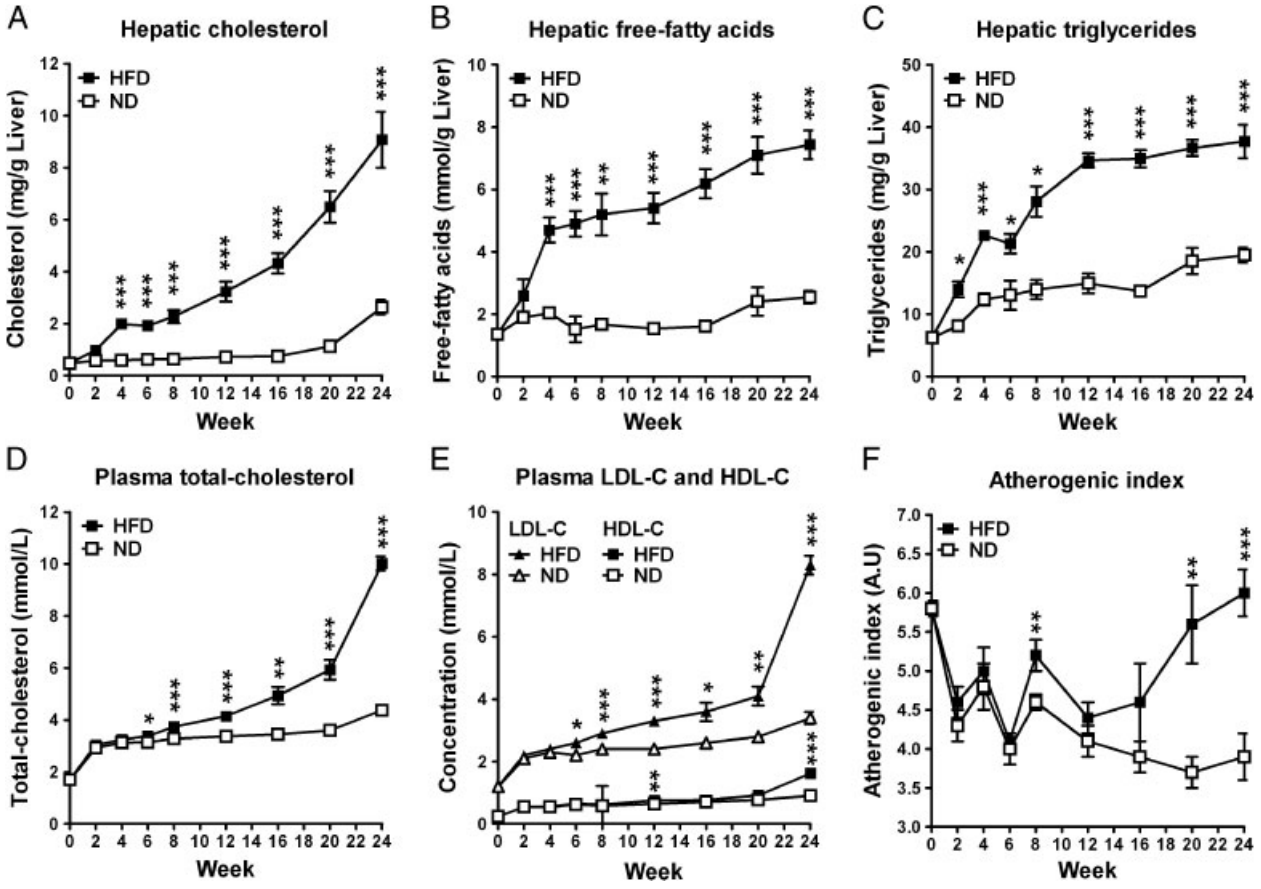

Figure 4. Time-dependent effect of a HFD on (A) hepatic cholesterol, (B) hepatic free-fatty acids, (C) hepatic triglycerides, (D) plasma total cholesterol, (E) Plasma LDL-C and HDL-C and (F) Atherogenic index over 24 weeks. LDL-C and AI were calculated as (Total-C)-(HDL-C)-(Triglycerides/5) and (Total-C)-(HDL-C)/HDL-C respectively. Data shown as mean ± SE. Significant differences between HFD versus ND are indicated. $^{*}p<0.05$. $^{**}p<0.01$. $^{***}p<0.001$. ND, normal diet; HFD, high-fat diet.

4.1 Early accumulation of hepatic FFA and TG

Liver morphology revealed early and progressive lipid droplet accumulation in the HFD group, indicating the early stages of fatty liver development. Hepatic injury may occur when the capacity of hepatocytes to store excess FFA is exceeded. In the HFD-fed mice, there was a time-dependent augmentation of hepatic FFA and TG levels. After 2 wk, hepatic TG were significantly elevated in the HFD group and coincided with the appearance of lipid droplets. Plasma FFA and TG concentrations were observed to be unaltered in the HFD group, similar to past studies on C57BL/6J mice fed an HFD [36]; however, the cause for the discrepancy between hepatic and plasma FFA concentrations is unknown at present.

Hepatic steatosis and lipotoxicity is primarily due to FFA accumulation rather than TG stored in lipid droplets [37]. Lipid droplet formulation may be a protective mechanism to prevent the accumulation of lipotoxins. In the HFD-fed mice, the accumulation of hepatic FFA and TG appears to be responsible for the time-dependent downregulation of not only β-oxidation but also FA and TG synthesis, indicated by the changes in hepatic enzyme activity. The suppression of FA synthesis in the HFD group is consistent with the downregulation of FA biosynthesis genes, which may partly explain the alterations in lipid homeostasis.

4.2 Time-dependent transcriptional activation of acute phase response and inflammation genes

Past studies in HFD-fed mice suggest an early induction of inflammation associated genes in liver [9]. Genes encoding acute phase reaction proteins were augmented after 2 wk in the HFD group and were elevated consistently over 24 wk. Microarray profiling revealed *Cidea*, a cell death-inducing DNA fragmentation factor-like effector was upregulated in the HFD-fed mice. *Cidea* is associated with lipid droplet accumulation and insulin sensitivity in humans [38]. Furthermore, *Cidea* has been linked to dysregulation of lipid metabolism and is a negative regulator of apoptosis. In hepatocytes, *Cidea* is necessary for *SREBP-1c* activated lipid accumulation and TG storage [39]. In HFD-fed mice, there is an early induction

Table 1. Time-course changes of hepatic lipid-regulating enzyme activities in HFD C57BL/6J obese mice

	Diet	Week 0	Week 2	Week 4	Week 6	Week 8	Week 12	Week 16	Week 20	Week 24
CPT†	ND	8.8±1.2	9.6±0.7	12.6±0.5	14.5±0.5	12.5±0.7	12.5±0.2	12.0±1.6	14.7±0.7	12.6±1.2
	HFD		11.6±0.5*	12.3±0.4	11.6±0.7**	10.3±0.4**	9.6±1.2*	8.8±0.7	7.6±0.4***	8.1±0.7**
β-oxidation†	ND	0.27±0.0	0.36±0.0	0.64±0.0	0.57±0.1	0.37±0.0	0.45±0.1	0.33±0.	0.35±0.0	0.59±0.1
	HFD		0.33±0.0	0.45±0.0**	0.34±0.1**	0.22±0.0**	0.23±0.0***	0.15±0.0***	0.19±0.0***	0.23±0.0***
G6PD†	ND	1.6±0.0	8.1±0.3	10.6±0.8	7.6±0.6	6.9±0.3	12.8±0.5	11.4±0.9	8.1±0.4	9.1±0.4
	HFD		2.1±0.2***	3.1±0.4***	2.8±0.1***	2.9±0.2***	2.2±0.1***	2.4±0.2***	2.4±0.2***	3.5±0.3***
ME†	ND	16.2±1.3	22.1±0.6	27.5±1.8	21.9±0.6	31.6±1.1	19.5±0.9	22.2±1.4	19.4±0.3	23.9±1.0
	HFD		10.0±0.5***	14.8±0.9***	13.0±1.4***	18.7±1.1***	22.2±1.3	22.9±2.2	21.1±0.9	22.5±1.3
PAP†	ND	4.3±0.5	5.2±0.3	4.4±0.2	4.8±0.2	4.7±0.2	4.9±0.3	5.8±0.2	5.8±0.3	4.0±0.4
	HFD		3.6±0.2***	3.2±0.1***	3.6±0.2***	3.7±0.2***	3.5±0.2**	4.2±0.4**	3.7±0.3***	3.7±0.2
ACAT††	ND	44.8±5.0	49.0±2.2	47.7±3.1	49.8±1.9	41.2±2.7	20.0±0.8	19.6±0.9	17.6±0.7	15.8±1.0
	HFD		50.1±3.5	66.5±3.9**	56.8±2.0*	41.4±1.3	32.8±1.1*	24.6±0.8*	21.0±0.8	19.6±0.2*
HMGR††	ND	193.0±14.1	244.2±14.3	230.2±4.9	228.7±17.3	204.8±12.4	165.9±13.9	121.3±10.8	107.0±19.0	109.7±5.2
	HFD		200.2±7.9*	160.8±12.4*	123.7±12.3**	171.9±7.0*	154.1±4.7*	106.0±4.7*	109.0±2.6	106.7±5.8

Data shown as mean±SE. Units are †nmol/min/mg protein or ††pmol/min/mg microsomal protein. Significant differences between HFD versus ND are indicated by *t*-test. *$p<0.05$. **$p<0.01$. ***$p<0.001$. ND: normal diet; HFD: high-fat diet; CPT: carnitne palmitoyl transferse; FAS: fatty acid synthase; G6PD: glucose-6-phosphate dehydrogenase; ME: malic enzyme; PAP: phosphatidate phosphohydrolase.

Table 2. Time-course changes of hepatic antioxidant enzyme activities in high-fat fed C57BL/6J obese mice

	Diet	Week 0	Week 2	Week 4	Week 6	Week 8	Week 12	Week 16	Week 20	Week 24
SOD (unit/mg protein)	ND	21.6±1.1	25.6±0.7	29.9±1.1	28.8±0.7	39.5±1.8	27.2±0.7	22.3±0.6	26.8±0.9	26.4±0.9
	HFD		28.5±1.1	30.3±1.3	29.9±1.5	41.4±1.9	32.3±1.5*	32.0±1.7**	45.2±2.5***	38.7±0.8***
CAT (μmol/min/mg protein)	ND	3.4±0.2	2.5±0.1	2.3±0.1	1.9±0.1	2.7±0.1	1.9±0.1	2.1±0.1	2.0±0.1	1.99±0.1
	HFD		3.1±0.1**	2.5±0.1	2.1±0.1	2.8±0.1	2.3±0.1**	2.7±0.2*	2.6±0.1**	2.16±0.1
GSH-Px (nmol/min/mg Hb)	ND	6.0±0.2	5.6±0.1	5.8±0.1	4.9±0.1	5.7±0.1	4.2±0.1	5.1±0.1	5.3±0.2	5.9±0.1
	HFD		6.1±0.1*	6.4±0.2*	4.9±0.1	6.1±0.2	5.2±0.1**	6.3±0.2***	6.7±0.2***	7.3±0.2***
TBARS (μmol/min/mg Hb)	ND	22.8±2.0	23.6±0.6	24.5±0.4	16.3±0.72	21.4±0.7	17.9±0.9	25.0±0.3	18.7±0.8	21.7±0.5
	HFD		25.0±0.7	23.4±0.5	18.5±1.04	22.9±0.5	22.8±0.6**	26.9±0.3**	20.4±1.4	18.5±0.3

Data shown as mean±SE. Significant differences between HFD versus ND are indicated by *t*-test. *$p<0.05$. **$p<0.01$. ***$p<0.001$. ND: normal diet; HFD: high-fat diet; SOD: superoxide dismutase; CAT: catalase; GSH-Px: glutathione peroxidase; GR: glutathione reductase; TBARS: thiobarbituric acid reactive substances.

Table 3. HFD responsive genes at multiple time-points in C67BL/6J mice

Time	HFD responsive genes		Top 10 HFD responsive genes at each time-point
2 wk	72↑	15↓	↑ Cfd, Lcn2, Saa3, Saa1, Ubd, Cxcl9, H2-Eb1, LOC641240, H2-Ab1, Cd52 ↓ Tsc22d3, Sqle, Fdps, Acot3, Apoa4, Lpin1, Acacb, Ugt1a12, Ugt1a5, Cyp17a1
4 wk	22↑	32↓	↑ Cfd, Saa3, Saa1, H2-Ab1, Gvin1, Cxcl1, Adam11, Mpeg1, S3–12, Gsta2 ↓ Cyp4a14, Fgf21, Lamb3, Acacb, Fdps, Acot3, Ugt1a5, D830014E11Rik, Apoa4, Cyp17a1
6 wk	88↑	23↓	↑ Cfd, Cxcl9, Saa3, Lcn2, Saa1, LOC667597, S3–12, Ubd, Gbp2, H2-Eb1 ↓ Usp18, Sqle, Cyp51, Dct, Clec2d, D830014E11Rik, Ugt1a12, Ugt1a5, Tff3, Cyp17a1
8 wk	130↑	18↓	↑ Cfd, Saa3, Lcn2, Saa1, Cxcl9, Ubd, Gsta1, Gbp2, LOC641240, H2-Eb1 ↓ Acacb, Sqle, Ugt1a12, Stard4, Mmd2, Apoa4, LOC666559, Ugt1a5, Fdps, Cyp17a1
12 wk	55↑	24↓	↑ Cfd, Cidea, Gsta1, S3–12, Ubd, Cxcl9, Saa3, Gpnmb, Saa1, Lcn2 ↓ Pltp, Ugt1a2, Acss2, Mmd2, LOC245892, LOC666559, Ctsa, Acacb, Fdps, Cyp17a1
16 wk	39↑	30↓	↑ Cfd, Cidea, Gsta1, S3–12, Krt23, D1Ertd471e, Cyp3a11, Lcn2, Gsta2, Anxa2 ↓ Ctsa, Stard4, Ugt1a5, Avpr1a, Tff3, Fabp5, LOC666559, LOC245892, Fdps, Cyp17a1
20 wk	52↑	29↓	↑ Cfd, Cidea, Gsta1, Gpnmb, Gsta2, Lcn2, Lpl, Saa1, Cyp2b13, S3–12 ↓ Clec2d, 2900060B14Rik, Ugt1a5, Fgf21, Cyp4a14, Acacb, Fdps, Hsd3b5, 1600032L17Rik, Cyp17a1
24 wk	128↑	35↓	↑ Gpnmb, Cfd, Lgals3, Lpl, Cidea, Ly6d, Anxa2, S100a11, Lyz2, Ubd ↓ Acss2, Cyp4a12b, Pcsk9, Sqle, Stard4, Acacb, Cyp17a1, LOC666559, Fdps, Hsd3b5
	241↑	91↓	Unique HFD responsive genes

Differentially expressed genes based on HFD vs ND comparison at each time-point, Benjamin-Hochberg adjusted *p*-value <0.05, FDR <5%, fold change >1. All differentially expressed genes (>1 fold change) at each time point are provided in Supporting Information 1. ↑, Top 10 up-regulated genes; ↓, Top 10 down-regulated genes. Unique HFD responsive genes were differentially expressed at one or more time points.

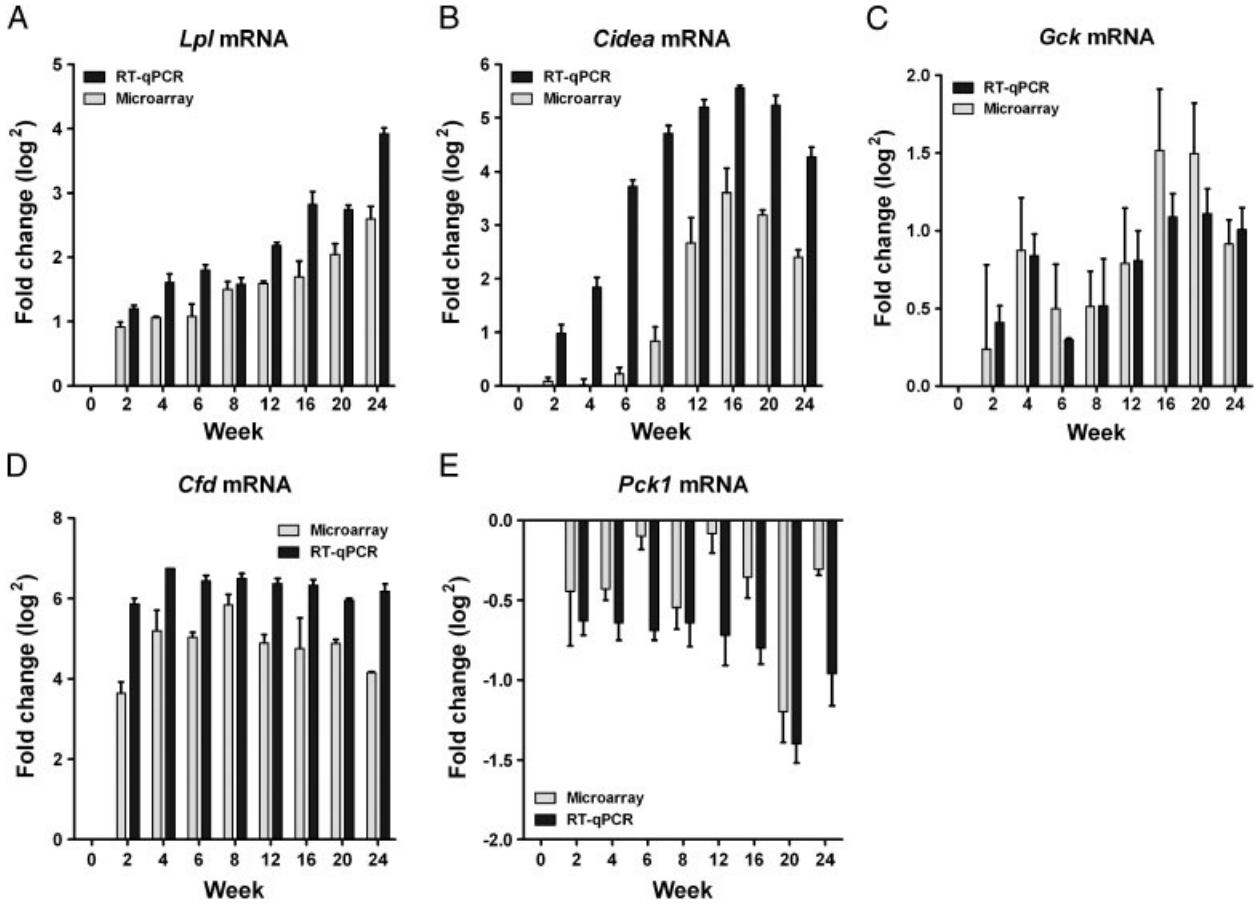

Figure 5. RT-qPCR validation of five HFD responsive genes based on microarray analysis. Fold changes in (A) *Lpl* mRNA, (B) *Cidea* mRNA, (C) *Gck* mRNA, (D) *Cfd* mRNA and (E) *Pck1* mRNA expression between HFD and ND fed mice at each time-point over 24 weeks. Data shown as mean ± SE.

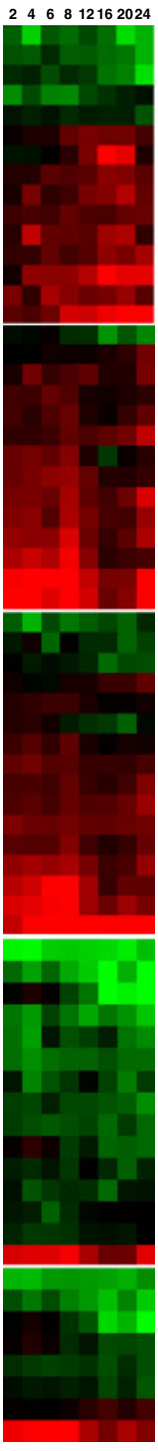

G	Terms	C	p-value
A	drug metabolism	13	7.17E-08
	metabolism of xenobiotics by cytochrome P450	12	1.68E-07
	retinol metabolism	12	2.30E-07
B	antigen processing and presentation	17	5.94E-13
	Systemic lupus erythematosus	15	4.73E-08
	Asthma	8	6.15E-06
	Chaperone mediated protein folding requiring	5	3.04E-05
	Allograft rejection	9	3.70E-05
	Autoimmune thyroid disease	9	6.00E-05
	Viral myocarditis	11	3.97E-05
C	defense response	36	8.49E-15
	inflammatory response	21	7.17E-10
	immune effector process	15	1.66E-08
	response to wounding	22	2.34E-07
	acute inflammatory response	11	1.02E-06
	adaptive immune response	11	1.02E-06
	lymphocyte mediated immunity	10	3.75E-06
	innate immune response	11	9.38E-06
	leukocyte mediated immunity	10	1.39E-05
D	lipid biosynthetic process	18	4.20E-06
	fatty acid metabolic process	14	9.76E-06
	carboxylic acid biosynthetic process	12	1.90E-05
	organic acid biosynthetic process	12	1.90E-05
	fatty acid biosynthetic process	9	5.00E-05
E	sterol metabolic process	9	3.46E-05
	steroid metabolic process	12	6.46E-05

Figure 6. (A) Functional gene ontologies associated with the HFD responsive genes. Functional gene ontology terms enriched among HFD responsive genes are clustered according to biological processes (enrichment score >2) using DAVID. The heatmap shows the expression profiles of the representative HFD responsive genes in each cluster.

of both pro-inflammatory and anti-inflammatory genes, as the liver attempts to maintain glucose and lipid homeostasis in the presence of high fat intake. In a previous study examining the time-course of global transcriptional changes in HFD-fed ApoE3L mice, an early upregulation of an inflammatory gene transcription program was reported, followed by a later transcriptional suppression of acute phase response genes [9, 10]. In the present study, we observed a consistent upregulation of inflammatory genes, but expression of acute phase response genes were still elevated after 24 wk in HFD-fed C57BL/6J mice. The initial trigger of the inflammatory response is unknown, but is likely to involve saturation of the β-oxidation pathway, leading to production of reactive oxygen species and an immune system response.

4.3 Time-dependent changes in oxidative stress markers

HFD can cause oxidative stress in liver, but the timing of oxidative stress induction is largely unknown. In the present study, the temporal profile of anti-oxidant enzyme activity suggested an early induction of hepatic CAT and GSH-Px activity followed by sustained activity between 12 and 24 wk coupled with augmentation of SOD activity. These findings suggest an adaptive response to protect against ROS production may occur in HFD-fed mice. TBARS an indicator of lipid peroxidation was elevated in HFD-fed mice between 12 and 16 wk, suggesting that excess dietary fat is directed toward lipid storage in liver. Transcriptional profiling revealed differential expression of cytochrome P450, glutathione transferase and glycosyltransferase genes. Recent studies suggest induction of ROS occurs early during HFD feeding in mice, but is repressed later [40]. The present findings suggest an early adaptive response occurs to protect against the deleterious effects of ROS, in agreement with other mouse models of obesity, including KKAy, *db/db* and DIO mice [41].

4.4 Time-dependent changes in hepatic cholesterol

Hepatic cholesterol accumulation occurred after 4 wk in the HFD-fed mice, but plasma total cholesterol was only significantly altered after 8 wk. Global transcriptional profiling revealed an early and sustained suppression of *Hmgcr* mRNA, which encodes a rate-limiting enzyme in cholesterol biosynthesis. Concomitant decreases in hepatic HMG-CoA activity were also observed, in agreement with a past study showing tight coupling between changes in transcription and HMG-CoA activity [42]. *Saa* genes that encode acute phase proteins and also promote cellular cholesterol efflux [43] were found to be upregulated in the HFD group. The cholesterol effux genes *Abcg5* and *Abcg8* were also upregulated in the HFD group. Cholesterol efflux genes encode proteins involved in reverse cholesterol transport from peripheral tissues, which results in increased hepatic cholesterol uptake and finally biliary/intestinal excretion [44]. *Hb* also plays a role in reverse cholesterol transport and was augmented late in the HFD-fed mice. Hence, genes involved in reverse cholesterol transport may represent attractive therapeutic targets to prevent hypercholesterolemia and atherosclerosis.

4.5 Time-dependent changes in insulin resistance and glucose tolerance

Insulin resistance and impaired glucose tolerance often occur in human obesity, although some obese individuals have remarkably normal insulin sensitivity [45]. In the HFD group, increased insulin resistance, elevated plasma insulin and impaired glucose tolerance were observed after 16 wk, while fasting plasma glucose was elevated later after 20 wk. Past studies show that HFD feeding induces insulin resistance more rapidly in the liver than in muscle or adipose tissue in animals and humans [46, 47].

The liver is a central regulator of glucose homeostasis and stores or releases glucose according to metabolic demands [48]. Insulin binds to receptors on the hepatocyte and results in inhibition of enzymes involved in gluconeogenesis and glycogenolysis, which are the primary sources of hepatic glucose production [49, 50]. G6Pase activity has been previously linked with the development of obesity, insulin resistance and T2D [51] although G6Pase activity was consistently suppressed in the HFD-fed mice after 16 wk. Hepatic GK activity, which catalyzes a key regulatory step of glycogen synthesis [52],] was increased after 16 wk in the HFD group, while glycogen levels were increased earlier after 12 wk. Transcriptional profiling revealed *Gck* expression was significantly increased in HFD group, and these findings were confirmed by RT-qPCR. In contrast, PEPCK activity was increased earlier after only 2 wk in HFD-fed mice. However, transcription of *Pck1* mRNA was consistently downregulated during the development of DIO, which suggests a post-transcriptional or allosteric mechanism modulates PEPCK activity.

Other hepatic genes modulated in HFD-fed mice, which may play a role in insulin resistance and impaired glucose metabolism, include *Mup* and *Lpin1*. *Mup* genes were downregulated after 20 wk in the HFD group. Recombinant *Mup1* has been shown to markedly attenuate hyperglycemia and glucose tolerance in HFD-fed diabetic mice [53]; however, the mechanism remains to be delineated. In other studies, *Lpin1,* which catalyzes the penultimate step in phosphoglycerol triacylglyceride synthesis, has been linked to insulin resistance [54]; interestingly, *Lpin1* has been reported to be suppressed in obese mice [55]. In the present study, *Lpin1* expression was decreased sharply in the HFD group after 2 wk. *Lpin1* primarily augments insulin resistance indirectly via TAG synthesis, which interferes with the hepatic insulin signaling pathway [54].

There is some debate about whether insulin resistance causes TG accumulation and hepatosis or whether TG accumulation is the trigger leading to increased insulin resistance. The present findings show lipid droplet formation was clearly visibly in the HFD-fed mice, long before the induction of insulin resistance. Therefore, TG accumulation appears to precede insulin resistance in HFD-fed C57BL/6J mice. Overall, the HFD-fed mice in the present study appeared to adapt to a long-term HFD over 24 wk, by increasing insulin secretion in response to increased insulin resistance. It was surprising there was no clear evidence of coordinated temporal changes in glucose regulating genes in the HFD-fed mice over 24 wk, which would explain the induction of insulin resistance. Nevertheless, hepatic FFA accumulation has been reported to be closely associated with hepatic insulin resistance in animal models [56] and diminished glucose utilization [57]. Therefore, FA and TG accumulation in combination with inflammatory changes appear

to be likely candidates for suppressing hepatic insulin signaling and contributing to hepatic insulin resistance and hence increasing the risk of T2D in HFD-fed mice.

In conclusion, the present study provided a time-dependent global transcriptional profile in mice fed an HFD, which may partly explain the metabolic and morphological changes in liver during the long-term development of DIO and its co-morbidities. In future, new approaches targeting HFD responsive genes and the metabolic profile could help ameliorate the deleterious effects of a long-term HFD and prevent the development of DIO and related complications.

This research was supported by the SRC program (Center for Food & Nutritional Genomics: grant number 2010-0001886) of the National Research Foundation (NRF) of Korea funded by the Ministry of Education, Science and Technology.

The authors have declared no conflict of interest.

5 References

[1] Kopelman, P. G., Obesity as a medical problem. *Nature* 2000, *404*, 635–643.

[2] Cummings, D. E., Schwartz, M. W., Genetics and pathophysiology of human obesity. *Annu. Rev Med.* 2003, *54*, 453–471.

[3] Guh, D. P., Zhang, W., Bansback, N., Amarsi, Z. et al., The incidence of co-morbidities related to obesity and overweight: a systematic review and meta-analysis. *BMC Public Health.* 2009, *9*, 88.

[4] Hertog, M. G., Kromhout, D., Aravanis, C., Blackburn, H. et al., Flavonoid intake and long-term risk of coronary heart disease and cancer in the seven countries study. *Arch. Intern. Med.* 1995, *155*, 381–386.

[5] Matsuzawa-Nagata, N., Takamura, T., Ando, H., Nakamura, S. et al., Increased oxidative stress precedes the onset of high-fat diet-induced insulin resistance and obesity. *Metab. Clin. Exp.* 2008, *57*, 1071–1077.

[6] Rocha, V. Z., Libby, P., Obesity, inflammation, and atherosclerosis. *Nat. Rev. Cardiol.* 2009, *6*, 399–409.

[7] Clark, J. M., Diehl, A. M., Hepatic steatosis and type 2 diabetes mellitus. *Curr. Diab. Rep.* 2002, *2*, 210–215.

[8] Grayson, M., Nutrigenomics. *Nature* 2010, *468*, S1.

[9] Radonjic, M., de Haan, J. R., van Erk, M. J., van Dijk, K. W. et al., Genome-wide mRNA expression analysis of hepatic adaptation to high-fat diets reveals switch from an inflammatory to steatotic transcriptional program. *PLoS One* 2009, *4*, e6646.

[10] Kleemann, R., van Erk, M., Verschuren, L., van den Hoek, A. M. et al., Time-resolved and tissue-specific systems analysis of the pathogenesis of insulin resistance. *PLoS One* 2010, *5*, e8817.

[11] Matsuzawa, N., Takamura, T., Kurita, S., Misu, H. et al., Lipid-induced oxidative stress causes steatohepatitis in mice fed an atherogenic diet. *Hepatology* 2007, *46*, 1392–1403.

[12] Fraulob, J. C., Ogg-Diamantino, R., Fernandes-Santos, C., Aguila, M. B. et al., A mouse model of metabolic syndrome: insulin resistance, fatty liver and non-alcoholic fatty pancreas disease (NAFPD) in C57BL/6 mice fed a high fat diet. *J. Clin. Biochem. Nutr.* 2010, *46*, 212–223.

[13] Kim, S., Sohn, I., Ahn, J.-I., Lee, K.-H. et al., Hepatic gene expression profiles in a long-term high-fat diet-induced obesity mouse model. *Gene* 2004, *340*, 99–109.

[14] Gregoire, F. M., Zhang, Q., Smith, S. J., Tong, C. et al., Diet-induced obesity and hepatic gene expression alterations in C57BL/6J and ICAM-1-deficient mice. *Am. J. Physiol. Endocrinol. Metab.* 2002, *282*, E703–E713.

[15] Bligh, E., Dyer, W., A rapid method of total lipid extraction and purification. *Can. J. Biochem. Physiol.* 1959, *37*, 911–917.

[16] Do, G.-M., Kwon, E.-Y., Kim, E., Kim, H.-S. et al., Hepatic transcription response to high-fat treatment in mice: microarray comparison of individual versus. pooled RNA samples. *Biotechnol. J.* 2010, *5*, 970–973.

[17] Hulcher, F. H., Oleson, W. H., Simplified spectrophotometric assay for microsomal 3-hydroxy-3-methylglutaryl CoA reductase by measurement of coenzyme A. *J. Lipid Res.* 1973, *14*, 625–631.

[18] Davidson, A. L., Arion, W. J., Factors underlying significant underestimations of glucokinase activity in crude liver extracts: physiological implications of higher cellular activity. *Arch. Biochem. Biophys.* 1987, *253*, 156–167.

[19] Alegre, M., Ciudad, C. J., Fillat, C., Guinovart, J. J., Determination of glucose-6-phosphatase activity using the glucose dehydrogenase-coupled reaction. *Anal. Biochem.* 1988, *173*, 185–189.

[20] Bentle, L. A., Lardy, H. A., Interaction of anions and divalent metal ions with phosphoenolpyruvate carboxykinase. *J. Biol. Chem.* 1976, *251*, 2916–2921.

[21] Carl, M. N., Lakshmanan, M. R., Porter, J. W., Fatty acid synthase from rat liver. *Methods Enzymol.* 1974, *35*, 37–44.

[22] Markwell, M. A., McGroarty, E. J., Bieber, L. L., Tolbert, N. E., The subcellular distribution of carnitine acyltransferases in mammalian liver and kidney. A new peroxisomal enzyme. *J. Biol. Chem.* 1973, *248*, 3426–3432.

[23] Lazarow, P., Assay of peroxisomal β-oxidation of fatty acids. *Methods Enzymol.* 1981, *72*, 315–319.

[24] Ochoa, S., in: Colowick, S. P., Kaplan, N. O. (Eds), *Methods Enzymology*, Academic Press, New York 1955, pp. 323–326.

[25] Pitkänen, E., Pitkänen, O., Uotila, L., Enzymatic determination of unbound D-mannose in serum. *Eur. J. Clin. Chem. Clin. Biochem.* 1997, *35*, 761–766.

[26] Wolfram, S., Raederstorff, D., Wang, Y., Teixeira, S. R. et al., TEAVIGO (epigallocatechin gallate) supplementation prevents obesity in rodents by reducing adipose tissue mass. *Ann. Nutr. Metab.* 2005, *49*, 54–63.

[27] Shapiro, D. J., Nordstrom, J. L., Mitschelen, J. J., Rodwell, V. W. et al., Micro assay for 3-hydroxy-3-methylglutaryl-CoA reductase in rat liver and in L-cell fibroblasts. *Biochim. Biophys. Acta.* 1974, *370*, 369–377.

[28] Gillies, P. J., Rathgeb, K. A., Perri, M. A., Robinson, C. S., Regulation of acyl-CoA:cholesterol acyltransferase activity in normal and atherosclerotic rabbit aortas: role of a cholesterol substrate pool. *Exp. Mol. Pathol.* 1986, *44*, 329–339.

[29] Marklund, S., Marklund, G., Involvement of the superoxide anion radical in the autoxidation of pyrogallol and a convenient assay for superoxide dismutase. *Eur. J. Biochem.* 1974, *47*, 469–474.

[30] Aebi, H., in: Bergmeyer, H. (Ed.), *Methods of Enzymatic Analysis*, Academic Press, New York 1986, pp. 673–684.

[31] Paglia, D. E., Valentine, W. N., Studies on the quantitative and qualitative characterization of erythrocyte glutathione peroxidase. *J. Lab. Clin. Med.* 1967, *70*, 158–169.

[32] Ohkawa, H., Ohishi, N., Yagi, K., Assay for lipid peroxides in animal tissues by thiobarbituric acid reaction. *Anal. Biochem.* 1979, *95*, 351–358.

[33] Schmittgen, T. D., Livak, K. J., Analyzing real-time PCR data by the comparative C(T) method. *Nat Protocol.* 2008, *3*, 1101–1108.

[34] Smyth, G. K., in: *Bioinformatics and Computational Biology Solutions using R and Bioconductor*, Springer, New York 2005, pp. 397–420.

[35] Huang, D. W., Sherman, B. T., Lempicki, R. A., Systematic and integrative analysis of large gene lists using DAVID bioinformatics resources. *Nat. Protoc.* 2009, *4*, 44–57.

[36] Gao, S., He, L., Ding, Y., Liu, G., Mechanisms underlying different responses of plasma triglyceride to high-fat diets in hamsters and mice: roles of hepatic MTP and triglyceride secretion. *Biochem. Biophys. Res. Commun.* 2010, *398*, 619–626.

[37] Malhi, H., Gores, G. J., Molecular mechanisms of lipotoxicity in nonalcoholic fatty liver disease. *Semin Liver Dis.* 2008, *28*, 360–369.

[38] Puri, V., Ranjit, S., Konda, S., Nicoloro, S. M. C. et al., Cidea is associated with lipid droplets and insulin sensitivity in humans. *Proc. Natl. Acad. Sci. USA.* 2008, *105*, 7833–7838.

[39] Wang, R., Kong, X., Cui, A., Liu, X. et al., Sterol-regulatory-element-binding protein 1c mediates the effect of insulin on the expression of Cidea in mouse hepatocytes. *Biochem. J.* 2010, *430*, 245–254.

[40] Eccleston, H. B., Andringa, K. K., Betancourt, A. M., King, A. L. et al., Chronic exposure to a high fat diet induces hepatic steatosis, impairs nitric oxide bioavailability, and modifies the mitochondrial proteome in mice. *Antioxid. Redox Signal.* 2010, doi:10.1089/ars.2010.3395.

[41] Furukawa, S., Fujita, T., Shimabukuro, M., Iwaki, M. et al., Increased oxidative stress in obesity and its impact on metabolic syndrome. *J. Clin. Invest.* 2004, *114*, 1752–1761.

[42] Hwa, J. J., Zollman, S., Warden, C. H., Taylor, B. A. et al., Genetic and dietary interactions in the regulation of HMG-CoA reductase gene expression. *J. Lipid Res.* 1992, *33*, 711–725.

[43] van der Westhuyzen, D. R., Cai, L., de Beer, M. C., de Beer, F. C., Serum amyloid A promotes cholesterol efflux mediated by scavenger receptor B-I. *J. Biol. Chem.* 2005, *280*, 35890–35895.

[44] Khera, A. V., Rader, D. J., Future therapeutic directions in reverse cholesterol transport. *Curr. Atheroscler. Rep.* 2010, *12*, 73–81.

[45] Pataky, Z., Makoundou, V., Nilsson, P., Gabriel, R. S. et al., Metabolic normality in overweight and obese subjects. Which parameters? Which risks? *Int. J. Obes.* 2011, 10.1038/ijo.2010.264.

[46] Brøns, C., Jensen, C. B., Storgaard, H., Hiscock, N. J. et al., Impact of short-term high-fat feeding on glucose and insulin metabolism in young healthy men. *J. Physiol.* 2009, *587*, 2387–2397.

[47] Kraegen, E. W., Clark, P. W., Jenkins, A. B., Daley, E. A. et al., Development of muscle insulin resistance after liver insulin resistance in high-fat-fed rats. *Diabetes* 1991, *40*, 1397–1403.

[48] Schattenberg, J. M., Schuchmann, M., Diabetes and apoptosis: liver. *Apoptosis* 2009, *14*, 1459–1471.

[49] Valverde, A. M., Burks, D. J., Fabregat, I., Fisher, T. L. et al., Molecular mechanisms of insulin resistance in IRS-2-deficient hepatocytes. *Diabetes* 2003, *52*, 2239–2248.

[50] Saltiel, A. R., Kahn, C. R., Insulin signalling and the regulation of glucose and lipid metabolism. *Nature* 2001, *414*, 799–806.

[51] Park, J., Rho, H. K., Kim, K. H., Choe, S. S. et al., Overexpression of glucose-6-phosphate dehydrogenase is associated with lipid dysregulation and insulin resistance in obesity. *Mol. Cell. Biol.* 2005, *25*, 5146–5157.

[52] Agius, L., Peak, M., Newgard, C. B., Gomez-Foix, A. M. et al., Evidence for a role of glucose-induced translocation of glucokinase in the control of hepatic glycogen synthesis. *J. Biol. Chem.* 1996, *271*, 30479–30486.

[53] Zhou, Y., Jiang, L., Rui, L., Identification of MUP1 as a regulator for glucose and lipid metabolism in mice. *J. Biol. Chem.* 2009, *284*, 11152–11159.

[54] Ryu, D., Oh, K.-J., Jo, H.-Y., Hedrick, S. et al., TORC2 regulates hepatic insulin signaling via a mammalian phosphatidic acid phosphatase, LIPIN1. *Cell Metab.* 2009, *9*, 240–251.

[55] Chen, Z., Gropler, M. C., Norris, J., Lawrence, J. C. et al., Alterations in hepatic metabolism in fld mice reveal a role for lipin 1 in regulating VLDL-triacylglyceride secretion. *Arterioscler. Thromb. Vasc. Biol.* 2008, *28*, 1738–1744.

[56] Teli, M. R., James, O. F., Burt, A. D., Bennett, M. K. et al., The natural history of nonalcoholic fatty liver: a follow-up study. *Hepatology* 1995, *22*, 1714–1719.

[57] Langhans, W., Role of the liver in the control of glucose-lipid utilization and body weight. *Curr. Opin. Clin. Nutr. Metab. Care* 2003, *6*, 449–455.

